Daytime Boundary Layer Evolution in a Deep Valley. Part II: Numerical Simulation of the Cross-Valley Circulation

TSUNEO KUWAGATA

Tohoku National Agricultural Experiment Station, Morioka, Japan

FUJIO KIMURA

Institute of Geoscience, Tsukuba University, Tsukuba, Ibaraki, Japan

(Manuscript received 17 June 1996, in final form 16 October 1996)

ABSTRACT

The thermally induced circulation in a deep valley during fair weather and weak synoptic wind conditions is simulated by a two-dimensional numerical model, in order to investigate the daytime planetary boundary layer evolution observed in the Ina Valley, a deep, two-dimensional valley in Japan. The numerical model can simulate the observed structure of the PBL fairly well, along with the daytime variations of the observed valley surface air temperature and surface pressure.

The numerical simulations suggest that the thermally induced cross-valley circulation creates a two-layer PBL structure. That is, a turbulent mixed layer develops due to sensible heating from the surface, reaching to heights of about 500–1000 m above the valley floor, while a *quasi–mixed layer* is formed above the turbulent mixed layer by the heat transport of the cross-valley circulation. The quasi–mixed layer is a new feature of the PBL. The upper limit of the quasi–mixed layer corresponds to the top of the cross-valley circulation, being somewhat higher than both sides of the mountains. The quasi–mixed layer can be clearly distinguished during the daytime in a deep valley having a depth of greater than about 1500 m. Since the quasi–mixed layer has a slightly stable stratification, the magnitude of the coefficient of vertical turbulence in this layer is much less than that in the turbulent mixed layer.

The results of the simulations reveal that the thermally induced cross-valley circulation transports heat from the mountainous regions to the central part of the valley, while water vapor is transported in the opposite manner. The potential temperature becomes horizontally uniform during the afternoon, except in the shallow layer of the upslope flow along the side slopes. On the other hand, the daytime distribution of specific humidity in the valley is rather complex, being affected not only by the cross-valley circulation, but also by the ambient wind along the direction of the cross valley. Water vapor tends to be accumulated over the mountainous regions during the daytime, resulting in the formation of cumulus clouds. Visible images observed by the NOAA satellite confirm the development of cumulus clouds over the mountainous regions in the Ina Valley during the afternoon.

1. Introduction

Over complex terrain, such as a mountainous area, thermally induced local circulations develop under fair weather conditions—that is, no clouds and weak synoptic winds. The thermally induced circulation influences the development of the daytime planetary boundary layer, and, as a result, the structure of the PBL strongly depends on the circulation. Over the past several years, many studies on the PBL evolution over mountainous areas have been made. For example, Bossert and Cotton (1994a,b) investigated the thermally driven regional-scale circulations over the mountainous terrain of Colorado. Kimura and Kuwagata (1993) examined the thermally induced circulation passing from a plain to a basin over a mountain range. Walko et al. (1992) conducted a large-eddy simulation of the convective boundary layer over hilly terrain.

As to the daytime PBL evolution in a valley, observational studies were conducted by Whiteman (1982), Müller and Whiteman (1988), and Sakiyama (1990), while theoretical studies using numerical models were made by Whiteman and McKee (1982) and Bader and McKee (1983, 1985). These studies revealed that the thermally induced cross-valley circulation plays an important role in the breakup of the temperature inversion and the formation of the convective boundary layer (CBL) in a valley under fair weather conditions. On the other hand, recent studies indicated that the thermally induced cross-valley circulation also contributes to the heat and water vapor transport in a valley. According to the theoretical study by Kimura and Kuwagata

Corresponding author address: Dr. Tsuneo Kuwagata, Tohoku National Agricultural Experiment Station, 4 Akahira, Shimo-Kuriyagawa, Morioka 020-01, Japan.
E-mail: kuwa@tnaes.affrc.go.jp

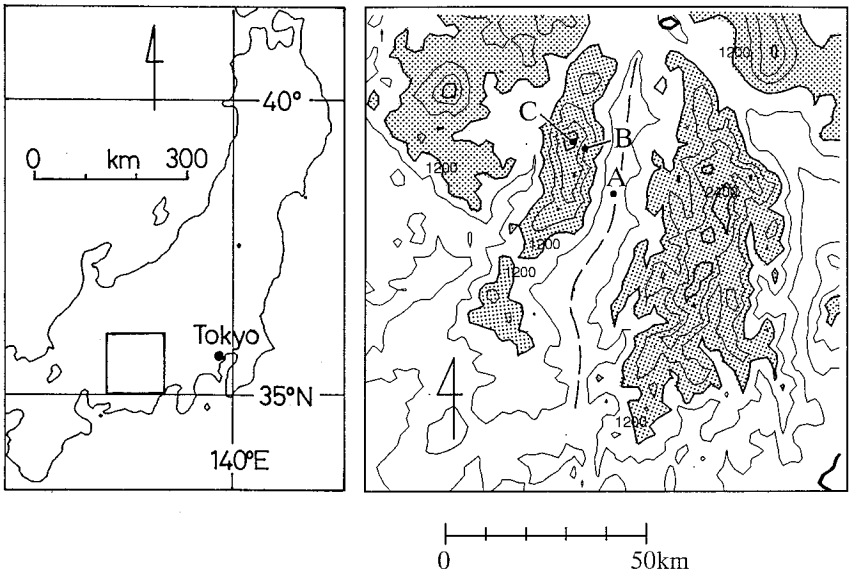

FIG. 1. Map of a part of Japan showing the location of the Ina Valley (left), and map of the Ina Valley corresponding to the area enclosed by the box in the left panel (right). The locations of the observational sites A, B, and C are indicated by letters, and the valley floor is indicated by the broken line. The contours indicate elevation (MSL) and are drawn with a 400-m interval. Shading denotes the area of elevation higher than 1200 m MSL.

(1995), heat is transported from the mountainous regions to the central part of the valley while water vapor is transported from the central part of the valley to the mountainous regions during the daytime and under fair weather conditions. That the heating rate of the PBL is larger at the valley bottom was confirmed by a heat budget analysis over central Japan during the daytime (Kondo et al. 1989; Kuwagata et al. 1990a,b).

In order to examine the contribution from the cross-valley circulation both to the structure of the PBL and to the heat and water vapor transport in a deep valley, the evolution of the daytime PBL was observed at the Ina Valley in Japan (Part I, Kuwagata and Kimura 1995). The Ina Valley is a deep, two-dimensional valley, having a width of about 40 km and a length of about 100 km (Fig. 1). The depth of the valley, which is the difference between the valley bottom and the top of the mountain ridges, ranges from 2000 to 2500 m. Observations were conducted at the three sites indicated by the letters A, B, and C in Fig. 1. Site A (Iijima) is the base site, located on the valley floor at an elevation of 690 m above mean sea level (MSL), where surface and upper-air meteorological data were gathered. Site B is located at an elevation of 1695 m MSL on the westward mountain slope, and site C is located at an elevation of 2645 m MSL near the top of the westward mountain; here, surface meteorological data were measured.

In the observation at the Ina Valley, Kuwagata and Kimura (1995) found the two-layer structure of the daytime PBL in a deep valley under fair weather and weak synoptic wind conditions. That is, the daytime PBL over the valley bottom consisted of two sublayers, a lower turbulent mixed layer and an upper sublayer having stable stratification. The two-layer structure of the PBL was also observed at the shallower basins or valleys that have depths of less than 1000 m (Whiteman 1982; Kondo et al. 1989). In the cases of the shallower basins or valleys, the upper sublayer merged with the lower turbulent mixed layer until the afternoon, resulting in a deeper CBL over the valley bottom. The upper sublayer observed in the Ina Valley, however, maintained a slightly stable stratification during the daytime and did not merge into the lower turbulent mixed layer, even in the late afternoon.

In the present study (Part II), the thermally induced circulation in a deep valley is simulated by a two-dimensional numerical model to clarify the mechanism of the formation of the two-layer structure of the daytime PBL observed in the Ina Valley. To add to that, the heat and water vapor transport in the Ina Valley due to the thermally induced circulation are also investigated.

2. The numerical model

According to the observed result, two-dimensional cross-valley circulation prevailed until the early afternoon in the Ina Valley (Kuwagata and Kimura 1995). Thus, the numerical model used in the present study is based on the two-dimensional Boussinesq equations employing the hydrostatic assumption with a terrain-following coordinate system. The governing equations and numerical scheme of the model are the same as those of the model developed by Kikuchi et al. (1981) and modified by Kimura and Arakawa (1983) and Kimura

and Manins (1988). The model is exactly the same as that used by Kimura and Kuwagata (1995), except for the parameterization of the momentum and heat exchange processes between air and land.

For simplification, the topography of the Ina Valley is simulated by a two-dimensional sinusoidal valley with periodic lateral boundaries. The depth of valley is set at 2000 m. The width of valley, which is the distance between the top of the mountains that form the sides of the valley, is set to 40 km. The top boundary of atmosphere is set at the height of 5500 m from the valley bottom. The steepness of the side slope in the model valley is $\sin\alpha = 0.1$ on average (α is the slope angle of the side slope). Both the Boussinesq and hydrostatic approximations employed in the present model are valid for simulating the daytime dry shallow convection, which has a depth of less than 3000 m in such a model valley (Pielke 1984).

The grid domain in the model consists of 40 grid points, located at a uniform horizontal interval of 1 km, and 119 vertical layers, with a smaller vertical interval in the lower layers. The top boundary is controlled by the wave radiation condition given by Klemp and Durran (1983) and Bougeault (1983) to avoid the reflection of gravity waves generated by local circulations in the lower layers. The vertical diffusion coefficients are estimated by the turbulent closure model (at level 2) developed by Mellor and Yamada (1974), where minimum values of the coefficients are set to 1 $m^2 s^{-1}$. Below the lowest vertical grid point, a constant flux layer is assumed. The height of the lowest vertical grid point above the ground ranges from 3.0 m (at the top of mountain) to 5.0 m (at the valley bottom).

The calculation procedures for the momentum and heat fluxes at the surface are somewhat different from those used by Kimura and Kuwagata (1995). That is, the momentum exchange between air and land is calculated by similarity theory for the surface boundary layer under neutral conditions. The time variations of the heat fluxes are given as boundary conditions without solving the surface heat balance since the present study is not focused on the heat exchange process between air and land.

The heat fluxes from the surface are given by

$$H = \frac{\pi}{2}\bar{H}\sin\left(\frac{\pi t}{t_e}\right) \tag{1}$$

and

$$lE = \frac{\pi}{2}\overline{lE}\sin\left(\frac{\pi t}{t_e}\right), \tag{2}$$

where H and lE are the sensible and latent heat fluxes, respectively; $t = 0$ is the time of sunrise; and $t = t_e$ the time of sunset. In addition, $\bar{H}$ and $\overline{lE}$ are the respective mean values of H and lE for $t = 0$ to t_e, and π is the circular constant. The time of sunrise, $t = 0$, is set to 0600 local time (LT) and t_e to 1800 LT. Values of $\bar{H} = \overline{lE} = 150$ W m^{-2} are assumed. The horizontal variations of the surface heat fluxes are thought to have been small during the present observations since there were no large changes in the ground surface and sunshine conditions in the valley. The heat fluxes are then assumed to have the same values for all sites in the valley. The exact values of H and lE were difficult to estimate in the Ina Valley during the observational period. In the previous study (Kuwagata et al. 1990b), the values of H and lE, averaged from 0600 to 1500 LT, were estimated as approximately 200 W m^{-2} in the Ina Valley, under fair weather conditions during the early summer season. The mean values of H and lE from 0600 to 1500 LT used in the present calculation are both 170 W m^{-2}.

TABLE 1. Parameters used in the numerical model.

Coriolis parameter	$f = 1.0 \times 10^{-4}$ s^{-1}
Surface roughness parameter	$z_0 = 0.2$ m
Density of atmosphere	$\rho = 1.0$ kg m^{-3}
Depth of valley	$D = 2000$ m
Width of valley	$W = 40$ km
Daytime mean sensible heat flux (from 0600 to 1800 LT)	$\bar{H} = 150$ W m^{-2}
Daytime mean latent heat flux (from 0600 to 1800 LT)	$\overline{lE} = 150$ W m^{-2}
Ambient wind speed (along the direction of the cross valley)	$U = 0$–2 m s^{-1}

The numerical model is integrated from $t = 0$ to t_e, with initial conditions of horizontally uniform temperature and specific humidity profiles, and a constant synoptic (ambient) wind along the direction of the cross valley. The values of the parameters used in the calculation are listed in Table 1.

For analyzing the results of the calculations, the accumulated sensible and latent heating in the PBL, Q_H and Q_E, are respectively defined as

$$Q_H \equiv c_p \int_0^\infty \rho(T - T_0)\, dz \simeq c_p\rho \int_0^\infty (\theta - \theta_0)\, dz \tag{3}$$

and

$$Q_E \equiv l \int_0^\infty \rho(q - q_0)\, dz \simeq l\rho \int_0^\infty (q - q_0)\, dz \tag{4}$$

$$\equiv \frac{w'}{l\rho_w}, \tag{5}$$

where c_p is the specific heat of air at constant pressure; l the latent heat of water vaporization; T the temperature; θ the potential temperature; and q the specific humidity; while T_0, θ_0, and q_0 are the initial values of T, θ, and q at $t = 0$, respectively. Furthermore, w' is the increase of precipitable water and ρ_w the density of water. The advection of sensible and latent heat, $Q_{H\text{adv}}$ and $Q_{E\text{adv}}$, can be evaluated as

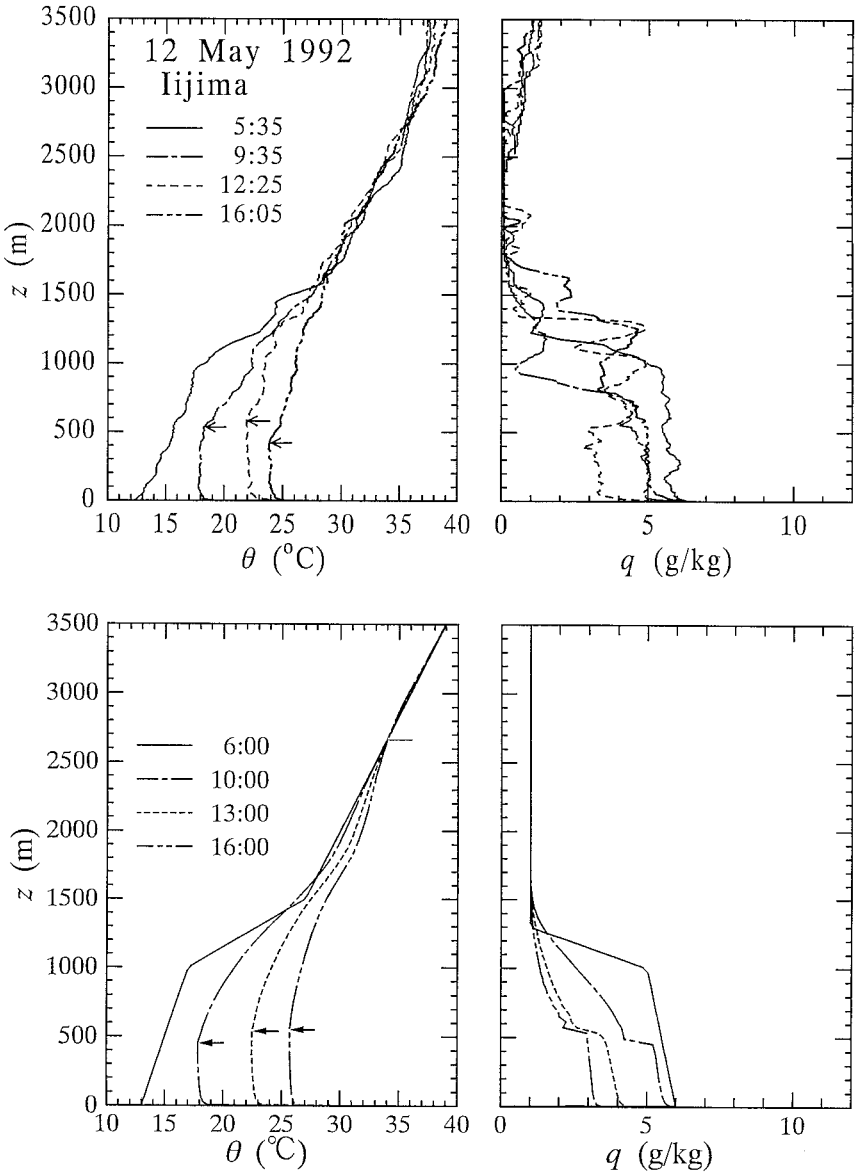

FIG. 2. Daily variations of the potential temperature (left) and specific humidity (right) profiles at the valley floor (site A) on 12 May 1992 (top is observed and bottom is calculated). The calculated values are the results for $U = 0$ m s^{-1} at the center of the valley. The tops of the turbulent mixed layer (lower sublayer) are indicated by arrows and those of the quasi–mixed layer (upper sublayer) by bars. Time corresponds to Japan standard time for the observed results and to local time for the calculated results.

$$Q_{H\text{adv}} = Q_H - \int_0^t H\, dt \tag{6}$$

and

$$Q_{E\text{adv}} = Q_E - \int_0^t lE\, dt. \tag{7}$$

It should be noted that these advection terms also include the contribution from the convergence of sensible and latent heat. The values of Q_H, Q_E, $Q_{H\text{adv}}$, and $Q_{E\text{adv}}$ can be calculated for each valley site.

In order to investigate the daytime heat and water vapor budgets in the PBL, the accumulated sensible and latent heating rates, averaged for 0600–1600 LT, are defined as $\langle Q_H \rangle \equiv Q_H^{16\text{LT}}/\Delta t$ and $\langle Q_E \rangle \equiv Q_E^{16\text{LT}}/\Delta t$. Here, $Q_H^{16\text{LT}}$ and $Q_E^{16\text{LT}}$ are the accumulated heating from 0600 to 1600 LT and $\Delta t = 10$ h. The daytime mean sensible and latent heat advection can also be defined as $\langle Q_{H\text{adv}} \rangle \equiv Q_{H\text{adv}}^{16\text{LT}}/\Delta t$ and $\langle Q_{E\text{adv}} \rangle \equiv Q_{E\text{adv}}^{16\text{LT}}/\Delta t$, respectively.

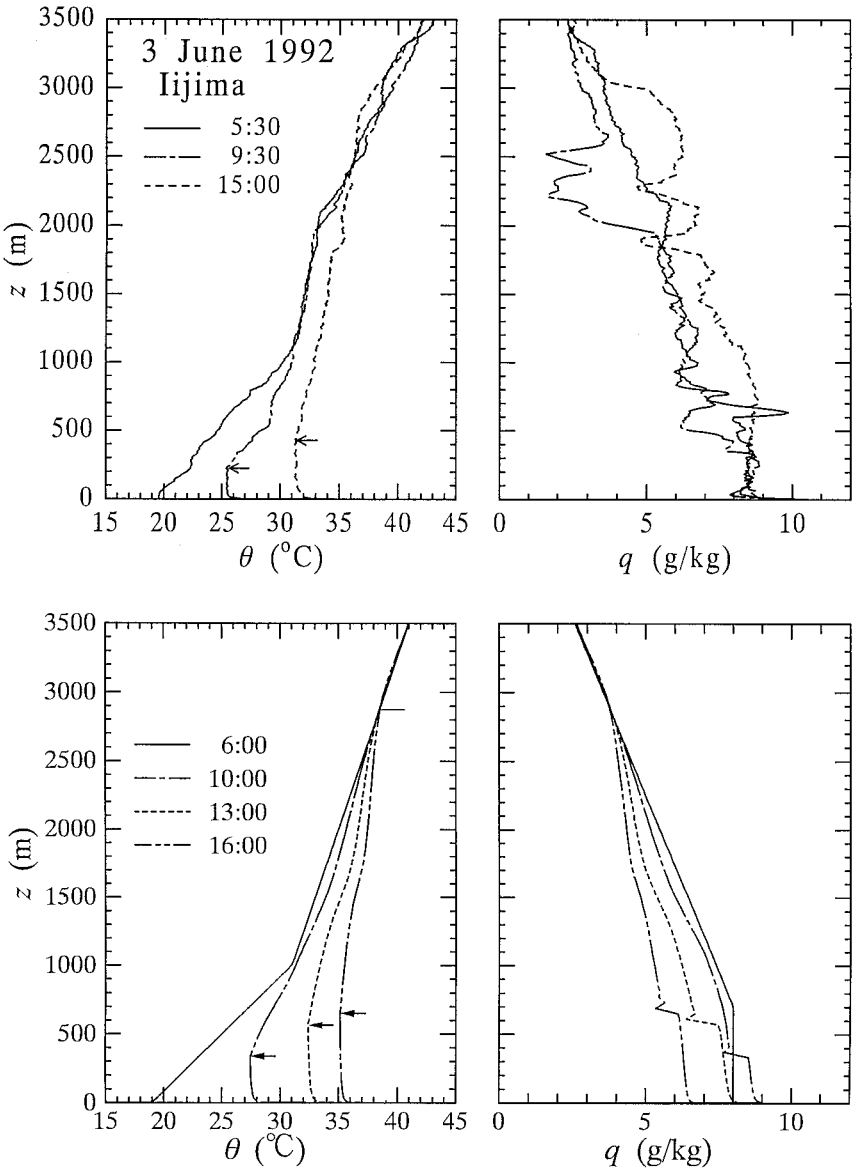

FIG. 3. As in Fig. 2 except for 3 June 1992.

3. Thermal structure of the PBL

a. The vertical structure of the PBL over the valley bottom

Figures 2 and 3 show the daily variations of the potential temperature (left) and specific humidity (right) profiles at the valley floor for 12 May and 3 June 1992, respectively (top is observed, and bottom is calculated at the center of the valley). Here, the ambient wind speed is set at $U = 0$ m s^{-1} for both calculations. The numerical model simulates the potential temperature profiles observed in the Ina Valley fairly well. The simulated structure of the PBL can be readily divided into two sublayers. The depth of the lower sublayer, termed the turbulent mixed layer, reaches about 500 m by the afternoon. The upper sublayer maintains a stable stratification during the daytime and gradually warms with time. According to the simulation, the top of the upper sublayer is found at 2600 to 2900 m above the valley floor, remaining invariant during the daytime and being somewhat higher than the height of the adjacent mountains (=2000 m). The upper sublayer is termed the *quasi–mixed layer* in the present study. The quasi–mixed layer is a new feature of the PBL.

Although the calculated values of specific humidity in the PBL decrease monotonically with time, the time variations of the observed specific humidity are rather complicated. The small maximum peaks observed in the quasi–mixed layer during the afternoon are not simulated by the numerical model. The specific humidity in

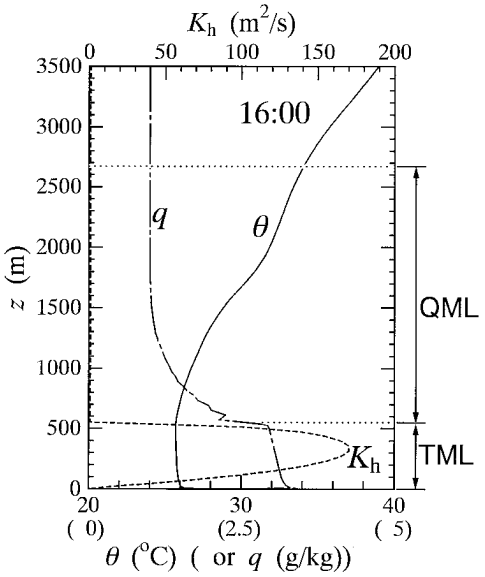

FIG. 4. The coefficient of vertical turbulence for heat K_h (dotted line) calculated by the numerical model at 1600 LT 12 May 1992, together with the simultaneous potential temperature (solid line) and specific humidity (chain line) profiles at the center of the valley for $U = 0$ m s^{-1} (TML: turbulent mixed layer, QML: quasi–mixed layer).

the turbulent mixed layer is vertically uniform in both the observed and calculated profiles.

The inconsistency of the specific humidity profile between that observed and that calculated is partly attributed to the advection by the ambient wind (which will be discussed in section 5b). The observed daytime mean wind speed component along the direction of the cross valley, averaged in the layer whose top is 3000 m above the valley bottom, was 2.1 m s^{-1} for 12 May 1992 and 1.0 m s^{-1} for 3 June 1992. Although the calculated profiles of specific humidity depend on the ambient wind speed U along the direction of the cross valley, those of potential temperature are almost the same for simulations of $U = 0$ to 2 m s^{-1} (not shown).

Figure 4 shows the coefficient of vertical turbulence for heat K_h, calculated by the numerical model at 1600 LT 12 May 1994, together with the simultaneous potential temperature and specific humidity profiles. The magnitude of K_h in the quasi–mixed layer is much less than that in the turbulent mixed layer, due to the characteristic stable stratification in the quasi–mixed layer. According to turbulent mixing, the potential temperature and specific humidity should become vertically uniform in the turbulent mixed layer. Specific humidity in the quasi–mixed layer, however, does not become vertically uniform, due to weak turbulent mixing.

b. The cross-valley circulation

Figures 5 and 6 show the cross sections of streamlines (top), potential temperature (middle), and specific humidity (bottom) in the valley at 1600 LT 12 May and 3 June 1992, respectively, calculated by the numerical model ($U = 0$ m s^{-1}). The layers of upslope flow along the side slopes of the mountains correspond to the turbulent mixed layer, having a depth of less than 500 m above the side slopes. The total depth of the thermally induced cross-valley circulation reaches heights of about 2600–2900 m above the valley floor, being 1.3–1.5 times as high as the depth of the valley.

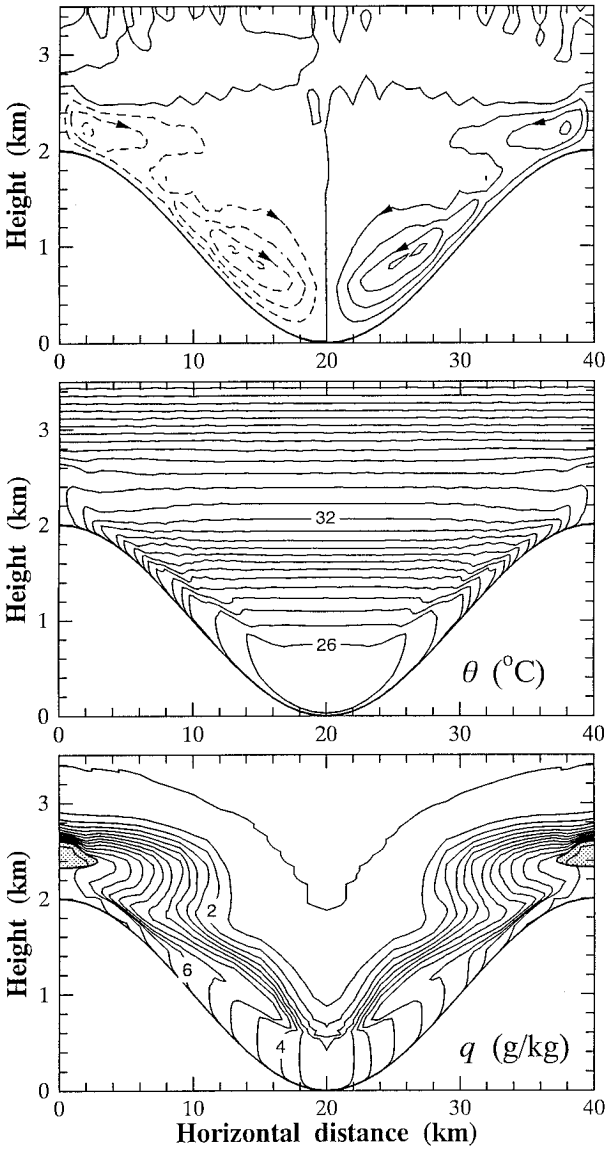

FIG. 5. Cross sections of streamlines (top), potential temperature (middle), and specific humidity (bottom) at 1600 LT 12 May 1992, calculated by the numerical model for $U = 0$ m s^{-1}. The streamline contour interval is 100 m^2 s^{-1}, that of potential temperature 0.5 K, and that of specific humidity 0.5 g kg^{-1}. The shaded areas (bottom) are the regions in which the calculated relative humidity exceeds 100%.

The potential temperature is horizontally uniform in the afternoon, except in the shallow layer of the upslope flow along the side slopes, being the result of the heat

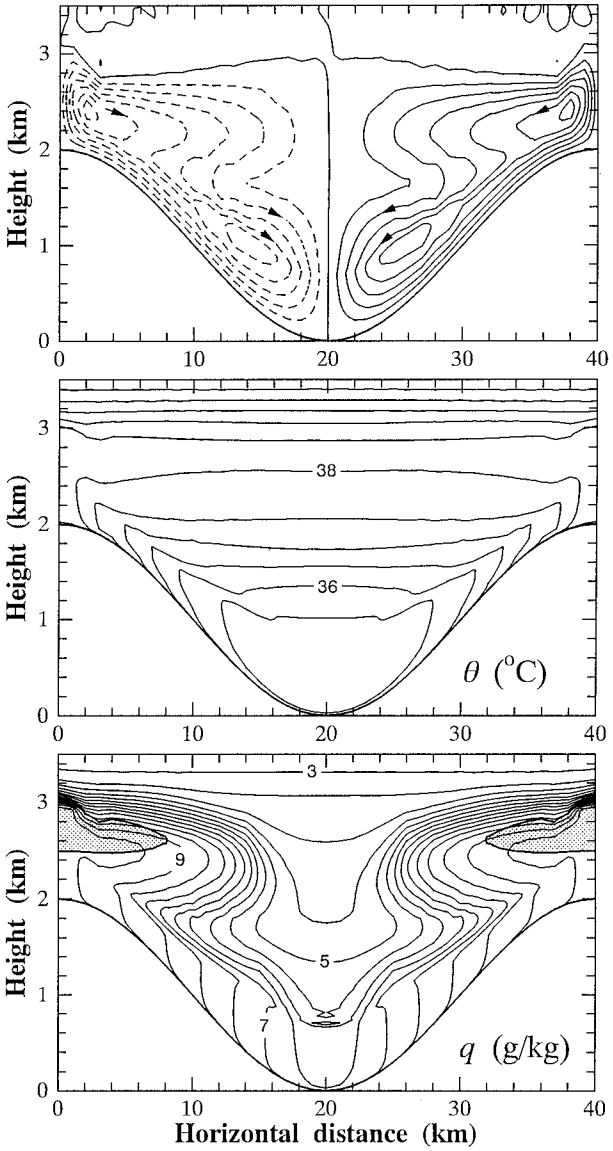

FIG. 6. As in Fig. 5 except for 3 June 1992.

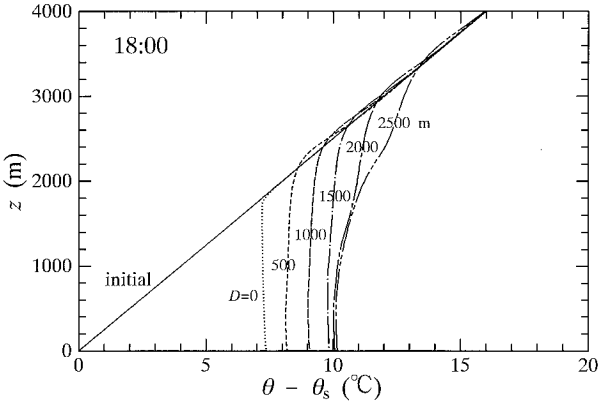

FIG. 7. Calculated potential temperature profiles at 1800 LT at the valley bottom for a valley depth of $D = 0$–2500 m. The vertical gradient of the initial potential temperature is set to 0.004 K m^{-1} at 0600 LT. The value of θ_s is the initial potential air temperature at the ground.

transport of the cross-valley circulation. The quasi–mixed layer corresponds to the counter part of the upslope flow, suggesting that the quasi–mixed layer is formed by the heat transport of the cross-valley circulation.

The specific humidity is not horizontally uniform in the afternoon. Water vapor is transported from the central part of the valley to the mountainous regions by the cross-valley circulation, resulting in the accumulation of latent heat over the mountains. That is, the specific humidity over the valley floor decreases due to the subsidence of dry air, while that over mountain ridges increases due to moist air advection from the bottom of the valley. Since the numerical model in the present study does not include the condensational process of water vapor, values of relative humidity are allowed to exceed 100%. As can been seen in the figures, the relative humidity over the mountain ridges exceeds 100% at 1600 LT.

c. Characteristics of the quasi–mixed layer

The daytime PBL in a deep valley consists of two sublayers, the lower turbulent mixed layer (TML) and the upper quasi–mixed layer (QML). On the other hand, as described in section 1, the two-layer structure of the PBL was also observed in the shallower basins or valleys that have depths of less than 1000 m only during the morning hours. Here, the vertical profiles of the PBL can be simulated by the numerical model for various valley depths. The parameters used in these simulations are the same as those described in section 2 (Table 1), except for the depth of the valley D and the vertical gradient of the initial potential temperature being set to 0.004 K m^{-1} at 0600 LT. Figure 7 shows the simulated potential temperature profiles at 1800 LT at the valley bottom for $D = 0$ to 2500 m. The QML can be clearly defined for a deep valley of $D \geq 1500$ m.

The QML can also be generated in shallower valleys of $D \leq 1500$ m. For a valley of $D \leq 1500$ m, although the QML can be clearly detected during the morning hours (not shown), it can not be distinguished from the lower TML during the afternoon. This result is consistent with the previous observations described above. In addition, the numerical simulation suggests that the structure of the PBL also somewhat depends on the width of valley W. The static stability of the QML in the late afternoon gradually increases with W if the width of valley ranges from 20 to 80 km (not shown).

According to the profile of the coefficient of vertical turbulence for heat (not shown), the depth of the TML is estimated as being 500–1000 m for a deep valley when $D \geq 1500$ m. On the other hand, the upper limit of the QML for $D \geq 1500$ m is roughly estimated as

TABLE 2. Characteristics of the turbulent mixed layer (TML) and the quasi–mixed layer (QML) in a deep valley ($D \geq 1500$ m). Here, D is the total depth of the valley and $\Gamma_d = 0.00976$ K m^{-1}.

	TML	QML
Height of the top of the layer from the valley floor	$h_{\mathrm{TML}} \simeq 500 \sim 1000$ m (gradually increasing during daytime)	$h_{\mathrm{QML}} \sim D + 1000$ m (invariant with time)
Static stability	Unstable ($-\partial\theta/\partial z \simeq \Gamma_d$)	Stable ($-\partial\theta/\partial z < \Gamma_d$) (static stability gradually decreasing with time)
Formation mechanism	Sensible heating from the surface	Heat transport by the thermally induced circulation

$D + 1000$ m above the valley bottom. The characteristics of the TML and QML for a deep valley can be summarized as listed in Table 2.

4. Heat transport due to the cross-valley circulation

a. Heat budget in the PBL

The thermally induced cross-valley circulation transports heat from the mountainous regions to the central part of the valley and, by doing so, adjusts the atmospheric available potential energy to a minimum value. The potential energy attains a minimum value for a valley having a width of less than 100 km (Kimura and Kuwagata 1995). As a result, the valley potential temperature is, for the most part, horizontally uniform in the afternoon. Figure 8 shows the daytime mean heat budget on 12 May 1992, as calculated by the numerical model. Here, the valley area is defined as the region in which the elevation of the ground surface is less than 1000 m from the valley floor, with the mountainous area defined as the residual region. The daytime mean sensible heat advection $\langle \hat{Q}_{H\mathrm{adv}} \rangle$ from the mountainous area to the valley is 135 W m^{-2} for $U = 0$ m s^{-1}. The calculated values of $\langle \hat{Q}_{H\mathrm{adv}} \rangle$ are almost the same for simulations of $U = 0$ and 1 m s^{-1}.

b. Time variations of the surface meteorological data

The heat transport calculated by the numerical model can be validated by the surface meteorological data observed at sites A, B, and C. Figure 9 shows the time variations of the surface air temperature on 12 May (top) and 3 June (bottom) 1992. The numerical model (solid circles and squares) simulates the surface air temperature observed at the valley floor (site A, solid line) and near the top of mountain (site C, dot–dash line) fairly well. The larger daytime increase of temperature at the valley floor and the smaller one over the mountainous region correspond to the difference in the daytime PBL heating rates between the two areas.

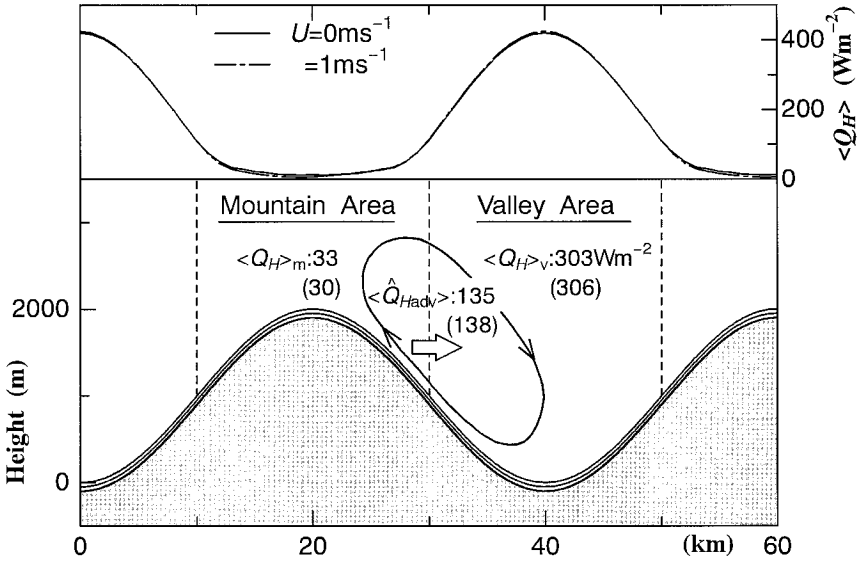

FIG. 8. The daytime mean PBL heat budget, calculated by the numerical model (0600–1600 LT 12 May 1992). The valley area is defined as the region in which the elevation of the ground surface is less than 1000 m from the valley floor, while the mountainous area is defined as the residual region. Values of $\langle Q_H \rangle_v$ and $\langle Q_H \rangle_m$ are the averaged values of the accumulated sensible heating rate over the valley and mountainous areas, respectively, and $\langle \hat{Q}_{H\mathrm{adv}} \rangle$ represents the sensible heat advection from the mountainous area to the valley area.

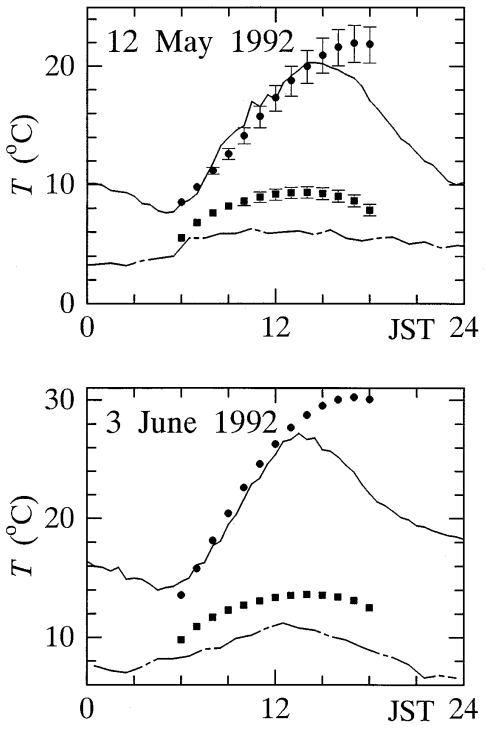

FIG. 9. Time variations of the valley surface air temperature on 12 May (top) and 3 June 1992 (bottom). Here, the solid and dot–dash lines are observed values at 3.7 m above the ground at site A (the valley floor) and at 1.5 m at site C (near the top of the westward mountain), respectively. The solid circles and squares indicate the calculated values at 5 m above the ground at the center of the valley and at 3 m above the ground at the top of mountain ($U = 0$ m s^{-1}), respectively. The range of the calculated values for $H = 120$ to 180 W m^{-2} is also indicated by the solid bars for 12 May 1992.

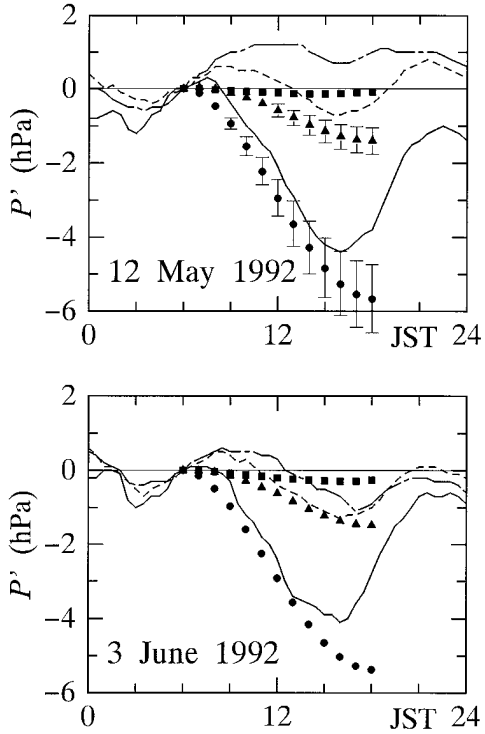

FIG. 10. Time variations of the valley surface pressure on 12 May and 3 June 1992. Here, the three lines represent observed values at site A (the valley floor, solid), site B (the slope of the mountain, broken), and site C (near the top of the westward mountain, dot–dash). The three solid symbols indicate the respective calculations for the same elevations for sites A, B, and C ($U = 0$ m s^{-1}). The range of the calculated values for $H = 120$ to 180 W m^{-2} is also indicated by the solid bars on 12 May 1992.

The observed temperature at the valley floor decreased after 1400 Japan standard time (JST), due to the cold-air advection from the southern coastal region by the up-valley wind along the valley floor (Kuwagata and Kimura 1995). The calculated temperature, however, gradually increases until 1800 LT since the two-dimensional numerical model does not simulate the advection due to the up-valley wind.

As described in section 2, the exact value of H in the Ina Valley was difficult to estimate during the observational period. The variation of the simulated temperature, indicated by solid bars in Fig. 9, was plotted if the value of the sensible heat flux H changed within the range of ±20%. The tops of solid bars for 12 May 1992 indicate the simulated temperatures for $H = 180$ W m^{-2}, while the bottoms of the bars indicate those for $H = 120$ W m^{-2}. As can be seen, the time variations of the simulated temperature are not very sensitive to the values of the sensible heat flux.

The time variations of the surface air pressure are shown in Fig. 10. According to Kuwagata and Kimura (1995), the surface pressure decreases in near proportion to the PBL heating rate if the atmospheric pressure at a certain level above the PBL remains invariant during the daytime. The numerical model (solid circles, triangles, and squares) simulates the surface pressure observed at the valley floor (site A, solid line), on the slope of the mountain (site B, broken line), and near the top of the mountain (site C, dot–dash line) fairly well. Larger decreases of surface pressure over the valley floor correspond to stronger heating rates of the PBL, while smaller decreases over the mountainous area correspond to weaker heating rates of the PBL. The increase of surface pressure observed over the valley floor after 1600 JST can be attributed to cold air advection by the up-valley wind.

In this section, we have presented the result of simulation for $U = 0$ m s^{-1}. The results for $U = 1$ and 2 m s^{-1} are almost the same as that for $U = 0$ m s^{-1} (not shown).

5. Water vapor transport due to the cross-valley circulation

a. Water vapor budget in the PBL

Figure 11 shows the daytime mean water vapor budget on 12 May 1992, calculated by the numerical model.

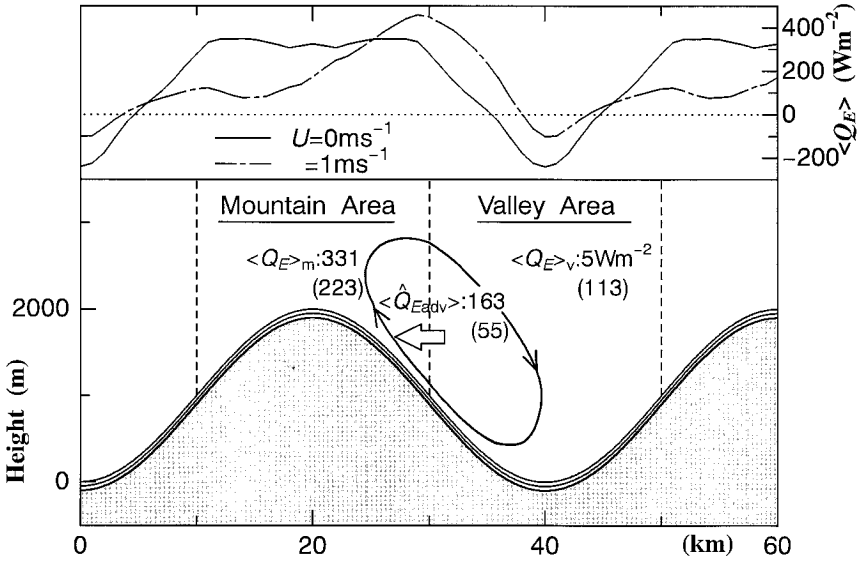

FIG. 11. The daytime mean PBL water vapor budget, calculated by the numerical model (0600–1600 LT 12 May 1992). Values of $\langle Q_E \rangle_v$ and $\langle Q_E \rangle_m$ are the averaged values of the accumulated latent heating rate over the valley and mountainous areas, respectively, and $\langle \hat{Q}_{Eadv} \rangle$ is the latent heat advection from the valley area to the mountainous area.

Water vapor is transported from the central part of the valley to the mountainous regions due to the thermally induced cross-valley circulation, resulting in latent heat accumulating over the mountainous regions. The daytime mean latent heat advection $\langle \hat{Q}_{Eadv} \rangle$ from the valley area to the mountainous area is 163 W m^{-2} for $U = 0$ m s^{-1} and 55 W m^{-2} for $U = 1$ m s^{-1}. The value of $\langle \hat{Q}_{Eadv} \rangle$ is somewhat affected by the ambient wind speed along the direction of the cross valley.

b. *Specific humidity over the valley bottom*

As described in section 3, the calculated values of specific humidity at the valley bottom (i.e., the center of the valley) are not consistent with those observed. According to the results of the numerical model (Figs. 5 and 6), the distribution of specific humidity in the valley is rather complex during the afternoon. Figure 12 shows the daily variations of the calculated specific

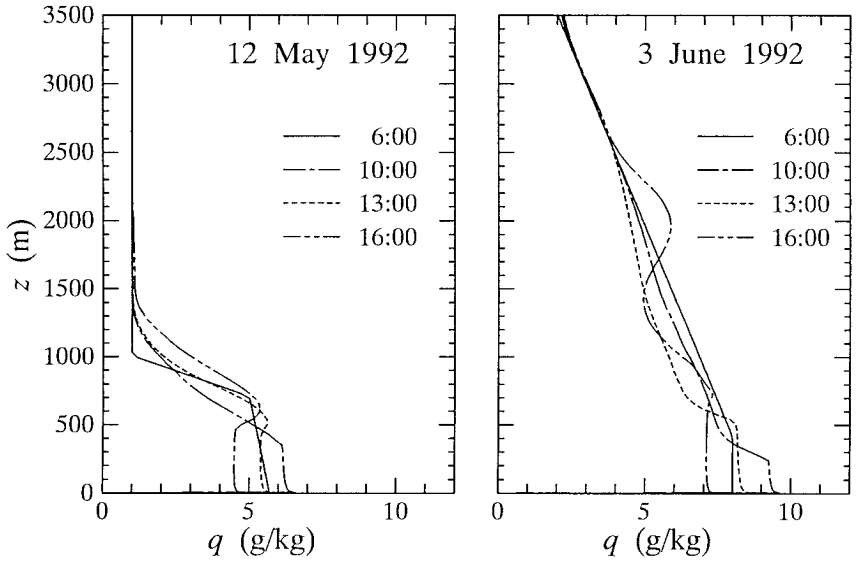

FIG. 12. Daily variations of the calculated specific humidity profiles at a model site 5 km from the center of the valley on 12 May (left) and 3 June 1992 (right). The times are indicated in the figure legends.

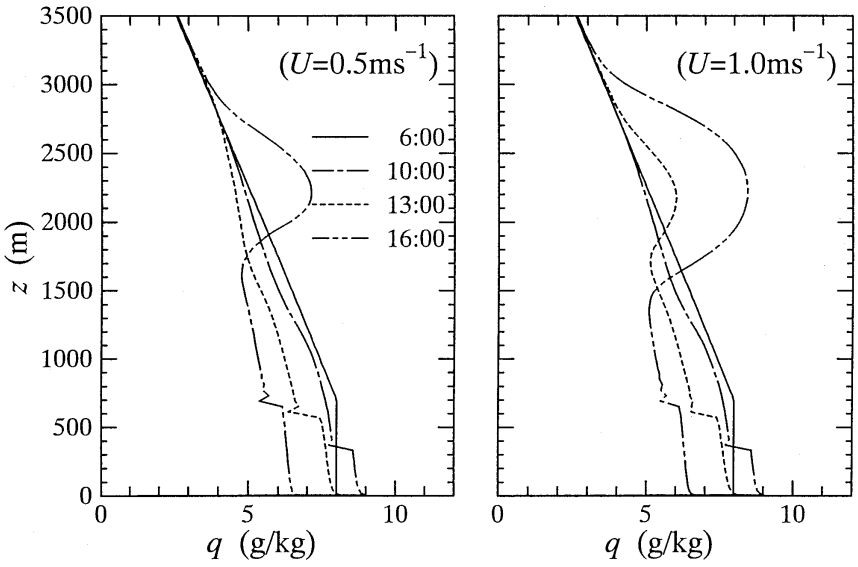

FIG. 13. Daily variations of the calculated specific humidity profiles at the valley bottom (i.e., the center of the valley) on 3 June 1992 for $U = 0.5$ m s^{-1} (left) and $U = 1$ m s^{-1} (right).

humidity profiles at a model site 5 km from the center of the valley for $U = 0$ m s^{-1}. The time variations of the specific humidity profile in the PBL are rather different from that at the center of the valley. Small maximum peaks, observed at the valley floor during the afternoon (Figs. 2 and 3), can be simulated.

As was shown in Fig. 11, the advection due to the ambient wind affects the specific humidity profile at the valley bottom. Figure 13 displays the daily variations of calculated specific humidity profiles at the valley bottom (the center of the valley) on 3 June 1992 for $U = 0.5$ and 1 m s^{-1}. The maximum afternoon peak around 2000–2500 m above the valley floor is simulated and is consistent with that observed. This peak results from moist-air advection from the mountainous regions by the ambient wind.

c. Time variation of accumulated latent heat

Water vapor transport by the cross-valley circulation results in the advection of dry air over the valley bottom. Figure 14 shows the time variations of the accumulated latent heat Q_E (the increase in precipitable water w') at the valley bottom. The calculated values of Q_E decrease monotonically during the daytime for $U = 0$ m s^{-1}, owing to dry air advection by the thermally induced cross-valley circulation. On the other hand, the values of Q_E begin to increase during the afternoon for both $U = 0.5$ and 1 m s^{-1}, which is attributed to moist-air advection by the ambient wind. Although the quantitative consistency is not very good between those observed and those calculated due to the complexity of the specific humidity field, the calculated time variations of Q_E exhibit a trend similar to those observed. The moist air advection by the up-valley wind also contributes to the increase of the observed Q_E during the evening hours, which cannot be simulated by the two-dimensional numerical model. The time variations of Q_E observed on 1 and 2 June 1992 exhibit similar features to those in Fig. 14 (not shown).

The latent heat transport due to the cross-valley circulation creates the accumulation of latent heat over the mountainous regions in the afternoon. That is, it can be expected that cumulus clouds will develop over the mountainous regions where supersaturation was simulated at 1600 LT (Figs. 5 and 6). Figure 15 displays the visible image (channel 2) of the area around the Ina Valley, observed by the Advanced Very High Resolution Radiometer (AVHRR) sensor of the National Oceanic and Atmospheric Administration (NOAA) satellite at 1407 JST 3 June 1992. This image reveals that cumulus clouds have developed over the mountainous regions.

6. Summary

The thermally induced circulation in a deep valley has been simulated by a two-dimensional numerical model, in order to investigate the daytime evolution of the observed PBL in the Ina Valley, a deep, two-dimensional valley in Japan. The simulations were conducted for fair weather and weak synoptic wind conditions. The structure of the PBL was found to be strongly affected by the thermally induced cross-valley circulation, with the numerical model simulating the observed circulation fairly well. The results are summarized as follows.

1) *The thermal structure of the PBL.* The daytime structure of the valley PBL is two-layered, consisting of a lower turbulent mixed layer and an upper quasi–

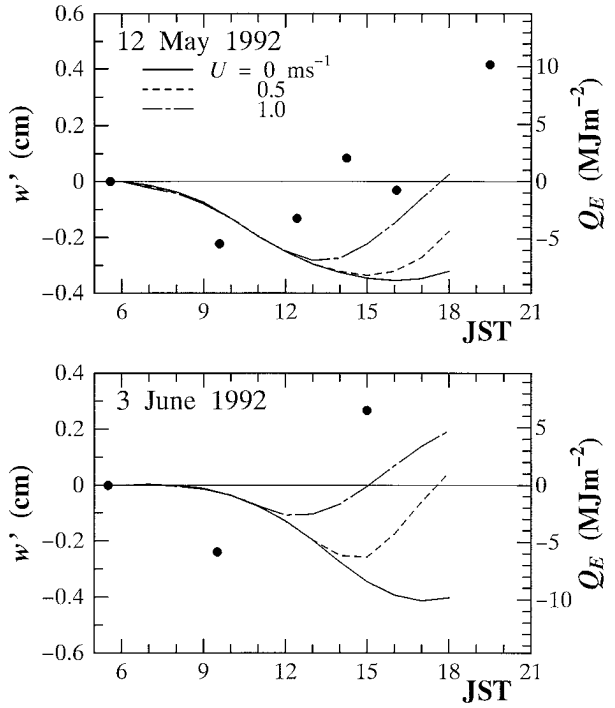

FIG. 14. Time variations of the accumulated latent heat Q_E (the increase of precipitable water w') at the valley bottom (solid circles are those observed, and lines are those calculated at the center of the valley). The figures are for conditions on 12 May 1992 (top) and 3 June 1992 (bottom).

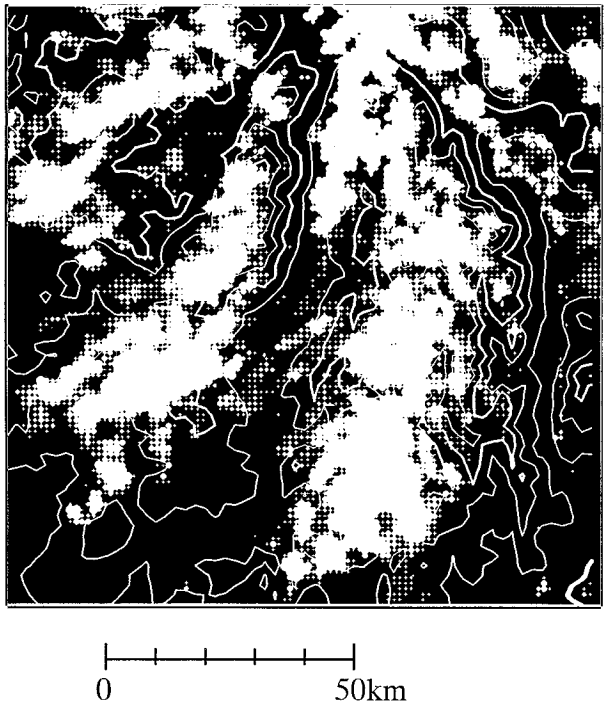

FIG. 15. Visible image (channel 2) of the area around the Ina Valley, observed by the AVHRR sensor of the NOAA satellite at 1407 JST 3 June 1992. The areas of cloud cover correspond to the white regions.

mixed layer. The turbulent mixed layer is created by sensible heating from the surface, reaching to heights of about 500–1000 m above the valley bottom by the afternoon. On the other hand, the quasi–mixed layer corresponds to the counterpart of the upslope flow, the top of which is somewhat higher than the top of the adjacent mountains. The quasi–mixed layer is heated by the heat transport of the cross-valley circulation, maintaining a slightly stable stratification. The magnitude of the coefficient of vertical turbulence in the quasi–mixed layer is much less than that in the turbulent mixed layer. The quasi–mixed layer is clearly distinguished until the late afternoon only in deep valleys having depths of over about 1500 m.

2) *Heat transport due to the cross-valley circulation.* The thermally induced cross-valley circulation transports heat from the mountainous regions to the central part of the valley. The potential temperature becomes horizontally uniform in the afternoon, except in the shallow layer of the upslope flow along the side slopes. The stronger PBL heating rate over the valley area results in a larger increase of surface air temperature and a larger decrease of surface pressure during the daytime. Conversely, the weaker PBL heating rate over the mountainous region results in a smaller increase of surface air temperature and a smaller decrease in surface pressure.

3) *Water vapor transport due to the cross-valley circulation.* The thermally induced cross-valley circulation transports water vapor from the central part of the valley to the mountainous regions. The transport of water vapor in a valley is also affected by the ambient wind along the direction of the cross valley. Water vapor tends to be accumulated over the mountainous region during the daytime, which results in the formation of cumulus clouds in the afternoon. The visible image observed by the NOAA satellite confirms the development of cumulus clouds in the afternoon over the mountainous regions of the Ina Valley, where supersaturation had been numerically simulated.

Acknowledgments. The authors would like to thank Prof. J. Kondo of Tohoku University for helpful discussions and useful advice, and also Prof. H. Kawamura of Tohoku University for providing the AVHRR data from the NOAA satellite. The two-dimensional graphplot tool, developed by Dr. K. Edamatsu of Tohoku University, was used in the drawing of the figures. The present study was partially supported by the Ministry of Education, Science, and Culture through Grant-in-Aid for Scientific Research 05640473.

REFERENCES

Bader, D. C., and T. B. McKee, 1983: Dynamic model of the morning boundary layer development in deep mountain valleys. *J. Climate Appl. Meteor.,* **22,** 341–351.

——, and ——, 1985: Effects of shear, stability and valley characteristics on the destruction of temperature inversions. *J. Climate Appl. Meteor.*, **24,** 822–832.

Bossert, J. E., and W. R. Cotton, 1994a: Regional-scale flows in mountainous terrain. Part I: A numerical and observational comparison. *Mon. Wea. Rev.*, **122,** 1449–1471.

——, and ——, 1994b: Regional-scale flows in mountainous terrain. Part II: Simplified numerical experiments. *Mon. Wea. Rev*., **122,** 1472–1489.

Bougeault, P., 1983: A non-reflective upper boundary condition for limited-height hydrostatic models. *Mon. Wea. Rev.*, **111,** 420–429

Kikuchi, Y., S. Arakawa, F. Kimura, K. Shirasaki, and Y. Nagano, 1981: Numerical study on the effects of on the land and sea breeze circulation in the Kanto District. *J. Meteor. Soc. Japan,* **59,** 723–738.

Kimura, F., and S. Arakawa, 1983: A numerical experiment of the nocturnal low level jet over the Kanto Plain. *J. Meteor. Soc. Japan,* **61,** 848–861.

——, and P. Manins, 1988: Blocking in periodic valleys. *Bound.-Layer Meteor.*, **44,** 137–169.

——, and T. Kuwagata, 1993: Thermally induced wind passing from plain to basin over a mountain range. *J. Appl. Meteor.*, **32,** 1538–1547.

——, and ——, 1995: Horizontal heat fluxes over a complex terrain computed using a simple mixed-layer model and a numerical model. *J. Appl. Meteor.*, **34,** 549–558.

Klemp, J. B., and D. R. Durran, 1983: An upper boundary condition permitting internal gravity wave radiation in numerical mesoscale models. *Mon. Wea. Rev.,* **111,** 430–444.

Kondo, J., T. Kuwagata, and S. Haginoya, 1989: Heat budget analysis of nocturnal cooling and daytime heating in a basin. *J. Atmos. Sci.,* **46,** 2917–2933.

Kuwagata, T., and F. Kimura, 1995: Daytime boundary layer evolution in a deep valley. Part I: Observations in the Ina Valley. *J. Appl. Meteor.,* **34,** 1082–1091.

——, M. Sumioka, N. Masuko, and J. Kondo, 1990a: The daytime PBL heating process over complex terrain in central Japan under fair and calm weather conditions: Part I. Meso-scale circulation and the PBL heating rate. *J. Meteor. Soc. Japan,* **68,** 625–638.

——, N. Masuko, M. Sumioka, and J. Kondo, 1990b: The daytime PBL heating process over complex terrain in central Japan under fair and calm weather conditions. Part II: Regional heat budget, convective boundary layer height and surface moisture availability. *J. Meteor. Soc. Japan,* **68,** 639–650.

Mellor, G. L., and T. Yamada, 1974: A hierarchy of turbulence closure models of planetary boundary layers. *J. Atmos. Sci.,* **31,** 1791–1805.

Müller, H., and C. D. Whiteman, 1988: Breakup of a nocturnal temperature inversion in the Dischma Valley during DISKUS. *J. Appl. Meteor.,* **27,** 188–194.

Pielke, R. A., 1984: *Mesoscale Meteorological Modeling.* Academic Press, 612 pp.

Sakiyama, S. K., 1990: Drainage flow characteristics and inversion breakup in two Alberta mountain valleys. *J. Appl. Meteor.,* **29,** 1015–1030.

Walko, R. L., W. R. Cotton, and R. A. Pielke, 1992: Large-eddy simulation of the effects of hilly terrain on the convective boundary layer. *Bound.-Layer Meteor.,* **58,** 133–150.

Whiteman, C. D., 1982: Breakup of temperature inversions in deep mountain valleys: Part I. Observations. *J. Appl. Meteor.,* **21,** 270–289.

——, and T. B. McKee, 1982: Breakup of temperature inversions in deep mountain valleys: Part II. Thermodynamic model. *J. Appl. Meteor.,* **21,** 290–302.